Mitigating Cladding-Induced Ripples in D-Band Polymer Microwave Fibers for Enhanced 6G Performance

Maria Jozwicka[#1], Gilles Callebaut[$2], Manuel Buehler[#], Martin Wagner[#], Ulf Huegel[#], Liesbet Van der Perre[$],

[#]HUBER+SUHNER AG, Switzerland

[$]KU Leuven, Belgium

[1]maria.jozwicka@hubersuhner.com, [2]gilles.callebaut@kuleuven.be

***Abstract* — Polymer Microwave Fibers (PMFs) are a promising solution for D-band communication in 6G systems, requiring a large bandwidth and low loss. However, inhomogeneities in the PMF cladding and launcher structures lead to unwanted mode propagation and reflections, causing ripples in the transmission coefficient that affect signal quality. This paper examines these cladding-induced ripples and explores the use of attenuation tape to mitigate their effects. The results demonstrate that the taped PMF reduces attenuation, minimizes ripples, and improves the coherence bandwidth by $4.5\,\mathrm{GHz}$, providing a more effective solution for high-bandwidth 6G communication than uptaped fibers.**

***Keywords* — polymer microwave fiber, 6G, D-band communication.**

I. Introduction

As mobile and video Internet usage soars, the demand for greater data capacity continues to rise. High throughput is vital for the efficiency of both current and next-generation wireless technologies. Motivated by the increasing demand for wide bandwidth, similar to 5G, 6G research is advancing towards the millimeter-wave spectrum [1]. In particular, the D-band $(110 - 170\mathrm{GHz})$ is being put in a spotlight due to its capability to support high data rate communication. The development of the D-band system solutions with the use of widely known mediums such as copper wirelines or optical fibers continues to progress [1]. Nevertheless, shifting towards higher frequencies imposes an increase in complexity and cost of prevalent hardware. Therefore, the development of new solutions is imperative.

Recently, a new 6G system approach, based on a radiostripe concept, was presented [2]. To facilitate this approach, a PMF [3] was chosen as the medium for the transfer of the RF signal between remote antenna units (Fig. 1). A polymer microwave fiber characterizes a relatively large bandwidth at D-band, low loss in comparison to copper and wireless links at $140\,\mathrm{GHz}$ [3] and integration capability with current CMOS mm-wave radios [4]. The operation in the D-band results in a reduction of the fiber cross-section. Consequently, the diameter of the fiber becomes comparable to that of existing copper and optical cables and is used as an alternative.

Despite the aforementioned advantages, certain PMF design challenges have to be addressed. One such challenge is the requirement for a protective, low-loss cladding surrounding the core. The constraint of low attenuation is currently being addressed by employing foamed polyethylene material as the cladding. This foamed cladding, however, exhibits inhomogeneity over the fiber length, presenting a significant drawback. The unsymmetrical profile of the cladding leads to excitement of undesired higher order modes and polarization with different propagation speed compared to the targeted propagation mode in the fiber. As a result, ripples can be observed in the transmission coefficient measurements. The ripples affect the clarity of the signal, necessitating more complex and computationally demanding post-processing methods. Therefore, improving the performance of the passive PMF component would be highly beneficial. This enhancement would eliminate the need for expensive and sophisticated active hardware, thus simplifying the overall communication system.

This paper presents a novel PMF cladding design aiming to reduce the requirements for complex signal processing hardware through improving the transmission properties of the polymer fiber. Section II focuses on the problem statement and analysis. In Section III, the fabrication of the fiber is presented. An experimental validation and discussion of the results are carried out in Section IV. Finally, Section V concludes the work.

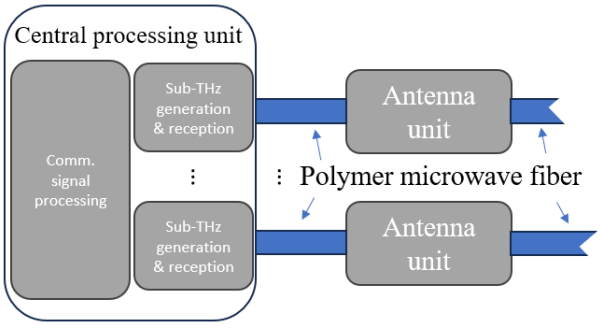

Fig. 1. Schematic representation of the radiostripe based communication concept.

II. Foam cladded PMF Analysis

As explored in [5], frequency-dependent attenuation and dispersion are critical limiting factors in PMF data transmission systems. These effects result in intersymbol

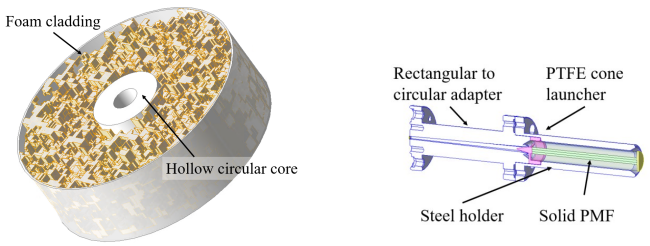

(a) (b)

Fig. 2. (a) Foam cladded PMF and (b) PMF launcher model

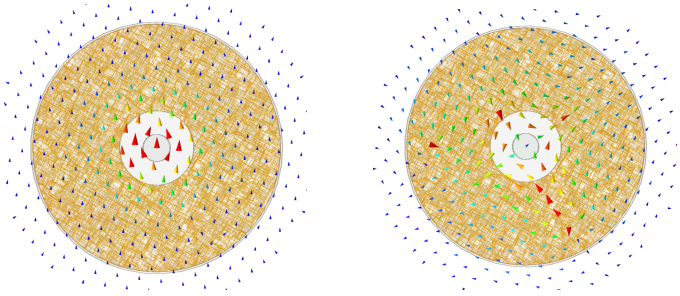

(a) (b)

Fig. 3. (a) HE_{11} desired and (b) Unwanted higher-order mode at 140 GHz.

interference (ISI), leading to signal degradation. To address dispersion-related challenges, fiber core design optimization methods have been proposed [6], [7]. However, another critical factor influencing the system performance, which has not yet been investigated, is the ripples in the transmission coefficient.

A. *Problem Statement*

The ripples in the transmission coefficient pattern are periodic variations resulting from standing waves within the fiber. These standing waves are generated by interference of the targeted propagation mode (HE_{11}) with undesired higher order or changed polarization modes traveling with different propagation speed on the waveguide. The amount of energy converting to a different mode or polarization may as well change the propagation direction - ending in reflections of the signal and local higher order mode resonances. The reflections of spurious cladding modes are induced by unsymmetrical dielectric value distribution in a cross-section of the fiber and by the PMF launcher itself.

To understand these effects, an elementary model of a small section of a PMF was created. To reduce dispersion, the hollow circular PMF core design was selected and optimized based on the mechanical constraints and guidelines provided in [6]. The optimized dimensions and selected materials are summarized in Table 1. Two factors contributing to ripple generation were investigated: 1) the foam cladding and 2) the PMF launcher.

1) *Foam Cladded PMF*

A detailed model of the complex structure of the foam cladding was created (Fig. 2a). The air bubbles in the foam were approximated as cube shapes (of random size and distribution) to simplify the meshing of the structure. Due to the model's complexity, only a lambda portion (2mm) was simulated. The simulation revealed that, although only the targeted first-order polarization mode (Fig. 3a) was launched, higher order modes (Fig. 3b) and other polarizations get exited by the inhomogeneity of the cladding. Such higher-order modes are more susceptible to reflections and can contribute to the ripples in the transmission coefficient.

2) *PMF Launcher*

The PMF launcher model is a rectangular-to-circular waveguide adapter featuring a polytetrafluoroethylene (PTFE) cone structure (Fig. 2b) designed to facilitate coupling with the

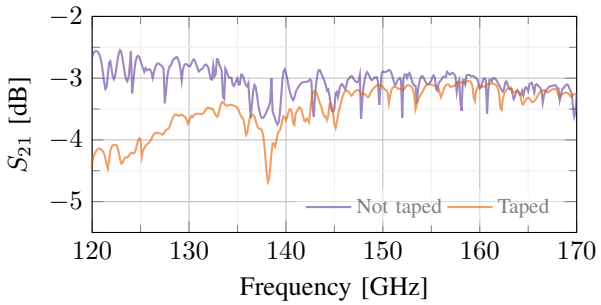

Fig. 4. Simulation of the launcher structure with a taped and untaped PMF.

PMF. A steel tube is incorporated to ensure precise alignment between the PMF and the cone. To reduce computational complexity and focus on the launcher's impact on ripple generation, the PMF is represented by a solid-cladding model with a dielectric constant of $\epsilon_r = 1.3$, approximating the behavior of the foam. The 'Not Taped' curve in Fig. 4 illustrates the results of the modeled inhomogeneous fiber. The presence of ripples of maximum 0.8 dB amplitude can be seen in the transmission coefficient, with an average insertion loss of 3 dB.

B. *Ripple Mitigation*

As presented, the inhomogeneous foam cladding of the PMF and the launcher lead to unwanted mode propagation and reflections, causing ripples in the transmission coefficient. To address this challenge and attenuate spurious modes, a novel approach was introduced by wrapping a nickel-chromium (NiCr) polyethylen tape around the cladding. The 'Taped' curve in Fig. 4 represents the launcher model simulation with the taped PMF. The findings demonstrate that this innovative method effectively attenuates spurious cladding

Table 1. Optimized dimensions and materials of a hollow circular core PMF.

	Core	**Cladding**
Material	PE	Foamed PE
ϵ_r	2.3	2.3
$\tan\delta$	$4E{-}4$	$4E{-}4$
$\boldsymbol{D}_{\text{out}}$	2.05 mm	5.50 mm
$\boldsymbol{D}_{\text{in}}$	0.40 mm	2.05 mm

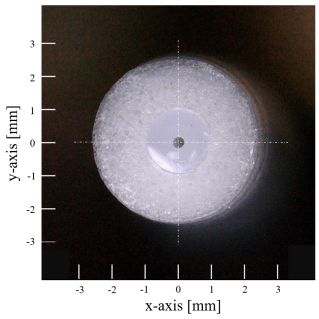

Fig. 5. Microscopic picture of the manufactured PMF.

modes and reduces reflections within the fiber. Thus, resulting in destructive interference and average ripple amplitude reduction of $0.5\,\mathrm{dB}$ in comparison to the untaped model. At lower frequencies (up to $140\,\mathrm{GHz}$), the taped model exhibits an average attenuation $1\,\mathrm{dB}$ lower than that of the untaped model. This reduction occurs because a larger portion of the electromagnetic wave propagates within the cladding at lower frequencies, where it is more effectively attenuated by the tape.

III. Manufacturing

The manufacturing of PMFs presents several challenges, particularly in ensuring the stability and uniformity of the core's cross-section along the fiber's length. In addition, maintaining the concentric alignment of the core within the cladding, as well as the hole within the core, is essential. The most reliable method to produce PMFs under these constraints is by using a coaxial cable extruder. In this process, a dielectric core and foam cladding are extruded directly onto a metal inner conductor, with the centricity of the metal conductor within the core continuously monitored via capacitive measurements at the extruder. After extrusion, the PMF is cut into 1m sections, and the metal inner conductor is removed, leaving a precisely aligned hole through the core.

Figure 5 shows a microscopic image of the manufactured PMF, highlighting the well-maintained concentricity of both the core and the hole (center-to-center deviation of less than 0.03mm). Moreover, the cross-section exhibits the required symmetrical and circular shape.

The PMF launcher, designed as a waveguide transition from a rectangular to a circular cross-section together with a tube section aligning the PMF, was fabricated using a computer numerical control (CNC) machining process. This approach ensured not only precise dimensional tolerances but also a high-quality surface finish, critical for minimizing signal losses and ensuring effective mode coupling.

IV. Measurement and Analysis

The measurements were carried out with a set-up shown in the Fig. 6. Two ports of the vector network analyzer (VNA) were calibrated using a two-port through-open-short-match (TOSM) routine in order to avoid systematic errors. The customized launchers, detailed in Section II, were employed to facilitate the transition from a rectangular to a circular waveguide. Measurements were first conducted on a $1\,\mathrm{m}$ section of untaped PMF, followed by taping the PMF with NiCr tape and repeating the measurements.

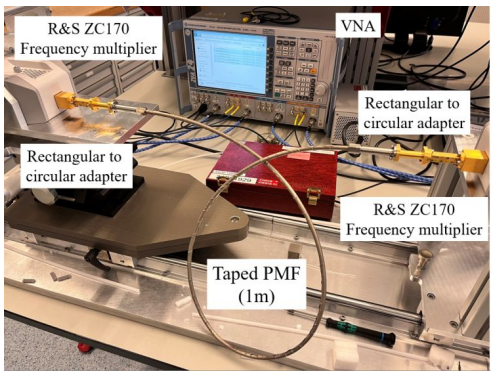

Fig. 6. Measurement set-up.

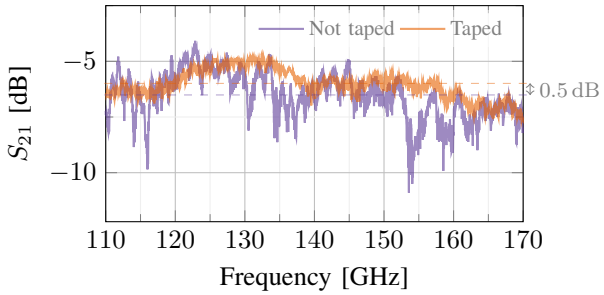

Fig. 7. Measured transmission coefficients. The taped fiber experiences less frequency selectivity and attenuates on average $0.5\,\mathrm{dB}$ less than the untaped fiber.

As illustrated in Fig. 7, the untaped fiber shows more fading dips compared to the taped fiber. Additionally, the frequency response dips are more pronounced in the untaped fiber. The untaped fiber has the smallest transmission coefficient (S_{21}) at $-10.9\,\mathrm{dB}$, which is $3.24\,\mathrm{dB}$ less than the lowest S_{21} value observed in the taped fiber. The untaped fiber has an average insertion loss which is $0.5\,\mathrm{dB}$ higher than the taped fiber. It can be noticed that the average insertion loss of the measurements is higher by $3\,\mathrm{dB}$ in comparison to the simulations. It is due to the losses induced by the second launcher which was not included in the simulations. In conclusion, the taped fiber is more robust and provides a lower attenuation with respect to the untaped fiber.

The receiver complexity and system performance depend on the coherence bandwidth of the full system and thus also the fiber. The coherence bandwidth is a statistical measure of the frequency range over which the channel frequency response can be considered flat or constant [8]. When the signal bandwidth is lower or equal than the coherence bandwidth of the system, the spectral components of a signal experience approximately equal gain and linear phase over that channel. However, when the transfer function varies across the system bandwidth, ISI occurs, necessitating equalization at the receiver before demodulation. Training symbols are employed to estimate the channel response and adaptively equalize the

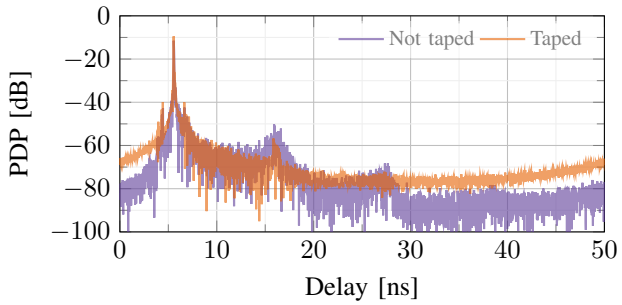

Fig. 8. Power delay profile (PDP) of both fibers.

signal. A larger coherence bandwidth reduces the amount of training symbols and filter taps, thereby lowering the receiver complexity and the computational load. In high-bandwidth sub-THz radio-over-fiber (RoF) systems, minimizing receiver complexity is particularly critical, especially at the user equipment (UE).

The coherence bandwidth can be studied by the frequency correlation function (FCF). The FCF is obtained by taking the Fourier transform of the PDP (Fig. 8), $R_c(\Delta F)$. The FCF is a measure of the normalized magnitude of the correlation between the channel response at two frequencies spaced by ΔF. The coherence bandwidth, is the bandwidth over which the FCF is above a certain threshold. Commonly, we use the following threshold: 0.5, 0.7 and 0.9, denoted by $B_{0.5}$, $B_{0.7}$, $B_{0.9}$, respectively.

The FCF of the two fibers under study and the coherence bandwidth gain are shown in Fig. 9 (left and right respectivelly). The coherence bandwidth gain is the difference between the bandwidth over which the FCF is above a certain threshold for the taped and untaped fiber. As indicated on the plot, the taped fiber improves the $B_{0.5}$, $B_{0.7}$ by respectively 4.5 and 1.4 GHz.

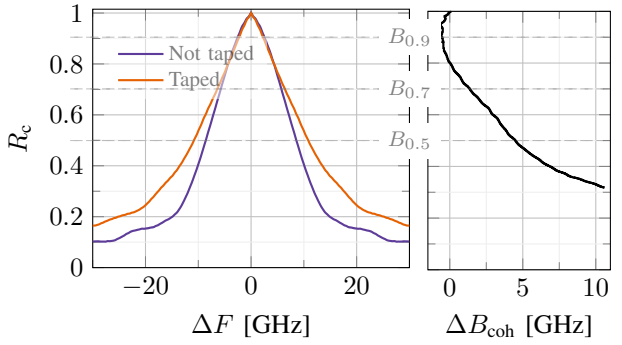

Fig. 9. Measured coherence bandwidth of both fibers. The difference between the coherence bandwidth of the taped and untaped fiber ΔB_{coh} is plotted at the right, i.e., how much coherence bandwidth is gained by taping the fiber for a given coherence value R_c.

V. Conclusion

A novel NiCr PMF cladding mitigating the transmission coefficient ripples is presented. An untaped and taped versions of the PMF are designed, manufactured and compared. From the perspective of communication, the taped fiber introduces less attenuation, has fewer, less extreme dips in the frequency response, and has a larger coherence bandwidth (more than 4.5 GHz) compared to the untaped fiber. These characteristics are detrimental when designing high-bandwidth communication systems, as envisioned for the next-generation and 6G networks.

Acknowledgment

6GTandem has received funding from the Smart Networks and Services Joint Undertaking (SNS JU) under the European Union's Horizon Europe research and innovation program under Grant Agreement No 101096302.

References

[1] T. Maiwald, T. Li, G.-R. Hotopan, K. Kolb, K. Disch, J. Potschka, A. Haag, M. Dietz, B. Debaillie, T. Zwick, K. Aufinger, D. Ferling, R. Weigel, and A. Visweswaran, "A Review of Integrated Systems and Components for 6G Wireless Communication in the D-Band," *Proceedings of the IEEE*, vol. 111, no. 3, pp. 220–256, 2023.

[2] E. Ernfors. (2019, Feb.) Radio stripes: re-thinking mobile networks. [Online]. Available: https://www.ericsson.com/en/blog/2019/2/radio-stripes

[3] M. De Wit, S. Ooms, B. Philippe, Y. Zhang, and P. Reynaert, "Polymer Microwave Fibers: A New Approach That Blends Wireline, Optical, and Wireless Communication," *IEEE Microwave Magazine*, vol. 21, no. 1, pp. 51–66, 2020.

[4] S. Ooms and P. Reynaert, "A Flexible Low-Latency DC-to-4 Gbit/s Link Operating from -40 to 200C in 28nm CMOS for Galvanically Isolated Applications," in *2018 IEEE Radio Frequency Integrated Circuits Symposium (RFIC)*, 2018, pp. 100–103.

[5] A. Meyer and M. Schneider, "Signal distortions in circular dielectric waveguides at mm-wave frequencies," *International Journal of Microwave and Wireless Technologies*, vol. 14, no. 1, p. 8–18, 2022.

[6] A. Meyer, K. Krüger, and M. Schneider, "Dispersion-Minimized Rod and Tube Dielectric Waveguides at W -Band and D -Band Frequencies," *IEEE Microwave and Wireless Components Letters*, vol. 28, no. 7, pp. 555–557, 2018.

[7] A. Standaert and P. Reynaert, "Analysis of Hollow Circular Polymer Waveguides at Millimeter Wavelengths," *IEEE Transactions on Microwave Theory and Techniques*, vol. 64, no. 10, pp. 3068–3077, 2016.

[8] A. F. Molisch, *Wireless communications: from fundamentals to beyond 5G*. John Wiley & Sons, 2022.